AN ACCELERATION SCHEME FOR BINARY STOCHASTIC MIXTURE DETERMINISTIC TRANSPORT EQUATIONS IN SLAB GEOMETRY

Brenton S. Ching
Puget Sound Naval Shipyard
1400 Farragut Ave.
Bremerton, WA 98314
ching@engr.orst.edu

Todd S. Palmer
Department of Nuclear Engineering
Oregon St. University
116 Radiation Center
Corvallis, OR 97331-5902
palmerts@engr.orst.edu

Keywords: stochastic mixtures, deterministic transport, iterative acceleration

ABSTRACT

Particle transport in stochastic mixtures has been an area of active research during the last decade. The primary focus has been on the development of simple, efficient models that approximate the behavior of transport solutions which have been ensemble-averaged over a large number of realizations of the mixing statistics. These approximate models are often written as coupled systems of transport equations. The stochastic nature of this problem can be naturally incorporated into Monte Carlo transport codes, but there have also been efforts to solve these coupled equations deterministically. In this paper, we develop an efficient iterative technique for the deterministic solution of the coupled transport equations of the Levermore-Pomraning mix model. The basis for its development is the observation that these equations are similar in structure to traditional multigroup transport equations with upscattering. We provide the results of a Fourier analysis of this technique, and compare these with observed convergence rates from the implemented algorithm.

1. INTRODUCTION

The transport of particles through stochastically mixed materials is important in a broad range of disciplines. In atmospheric sciences, radiative transfer through clouds is a stochastic mix transport problem. In nuclear engineering, two-phase coolant channels could be described with a stochastic mixture transport model. Radiation dose calculations in lung tissues may also benefit from these ideas.

The preponderance of the research in this area concerns the transport of particles through binary stochastic mixtures (BSM). There are two approaches to the solution of these problems. The first involves generating physical realizations of the statistics, solving the transport equation for these realizations, and then averaging the results to obtain the

ensemble average angular flux. For many problems, the solution of a single realization of the statistics, by either Monte Carlo or deterministic techniques, is very expensive, making this "brute-force" procedure computationally impractical.

A second approach involves averaging the transport equation itself, in an effort to directly generate equations for the ensemble-average flux. Most often, this approach leads to coupled systems of transport equations. Exact results can be obtained for purely-absorbing, time-independent problems in the special case of Markovian statistics, and for one-dimensional purely-scattering problems where the sources and scattering ratios are non-stochastic (Adams, Larsen and Pomraning, 1989). For general problems approximate models must be used. Much of the research in BSM transport has been in the benchmarking of these approximate models. Adams, Larsen and Pomraning (1989) compared the Levermore-Pomraning model, a simple coupled BSM transport model, with calculations made using the "brute-force" technique. Malvagi and Pomraning (1992) compared several BSM transport models in rod geometry with exact benchmark results. Su and Pomraning (1995) proposed a higher-order BSM transport model, which shows improved accuracy for transmission and reflecting probabilities, and for scalar flux distributions. Miller et al. (2001) have investigated the accuracy of several stochastic mix transport models when applied to the solution of radiative transfer problem with matter temperature coupling.

While there has been much effort expended to improve the accuracy of these BSM transport equations, little or no work has been done to find efficient ways of solving them. Ching and Palmer (2000) performed a Fourier analysis of three candidate Source Iteration (SI) schemes for the solution of the Levermore-Pomraning BSM model. This analysis shows that a fully-implicit treatment of the material interface coupling terms is stable, but can converge arbitrarily slowly for some problems. Miller, Rodrigue and Graziani (2001) have performed a similar analysis for SI applied to more sophisticated BSM transport models. In this paper, we develop and analyze a preconditioner for Source Iteration which appears to provide more rapid convergence for a wide variety of stochastic mix problems.

The remainder of this paper is organized as follows. In Section 2 we introduce the Levermore-Pomraning transport equations, and summarize the results of our previous work on iterative methods for these equations. In Section 3 we derive the proposed acceleration technique, mirroring the upscatter acceleration work of Adams and Morel (1993). We also include here a Fourier analysis of the acceleration, and compare these results with the convergence rates observed from the implemented algorithm. The low-order transport acceleration equations derived in Section 3 must also be solved iteratively, and if Source Iteration is used, this iteration can converge arbitrarily slowly. In Section 4, we derive a diffusion synthetic acceleration procedure for the "mixed" transport acceleration equations. This section also includes convergence rate predictions from Fourier analyses compared with observed data. Section 5 contains a discussion of our results and conclusions.

2. LEVERMORE-POMRANING BSM TRANSPORT MODEL

We are interested in solutions of the steady-state, monoenergetic transport equation in a slab geometry non-multiplying medium. The medium is composed of two materials, mixed randomly with known statistics. We focus specifically on the case of Markovian statistics, for which the Levermore-Pomraning BSM transport model becomes:

$$\mu\frac{\partial}{\partial x}p_1\psi_1(x,\mu)+\sigma_1(x)\,p_1\psi_1(x,\mu)=\frac{\sigma_{s1}(x)}{2}\int_{-1}^{1}d\mu' p_1\psi_1\left(x,\mu'\right) + \frac{|\mu|}{\Lambda_2}p_2\psi_2(x,\mu)-\frac{|\mu|}{\Lambda_1}p_1\psi_1(x,\mu)+p_1S_1, \tag{1}$$

$$\mu\frac{\partial}{\partial x}p_2\psi_2(x,\mu)+\sigma_2(x)\,p_2\psi_2(x,\mu)=\frac{\sigma_{s2}(x)}{2}\int_{-1}^{1}d\mu' p_2\psi_2\left(x,\mu'\right)$$
$$+\frac{|\mu|}{\Lambda_1}p_1\psi_1(x,\mu)-\frac{|\mu|}{\Lambda_2}p_2\psi_2(x,\mu)+p_2S_2. \tag{2}$$

The ensemble average angular flux is then simply the weighted average of the angular flux in each of the two materials:

$$\langle\psi(x,\mu)\rangle=p_1\psi_1(x,\mu)+p_2\psi_2(x,\mu). \tag{3}$$

Here, $p_i(x)$ is the probability that the location x is in material i, $\psi_i(x,\mu)$ is the ensemble averaged angular flux, given that position x is in material i, and Λ_i are the Markov transition probabilities. For homogeneous statistics, Λ_i is equal to the mean chord length in material i.

Ching and Palmer (2000) have analyzed three SI procedures for the deterministic solution of these equations. The fully-implicit SI procedure is described here, as are the results of a Fourier analysis of this scheme.

2.1 Source Iteration

Treating the material coupling terms implicitly is equivalent to guessing a scattering source in each of the two materials, and performing the transport sweeps in both materials simulanteously, as shown below:

$$\mu\frac{\partial}{\partial x}p_1\psi_1^{(\ell+1)}(x,\mu)+\sigma_1(x)\,p_1\psi_1^{(\ell+1)}(x,\mu)=\frac{\sigma_{s1}(x)}{2}\int_{-1}^{1}d\mu' p_1\psi_1^{(\ell)}\left(x,\mu'\right)$$
$$+\frac{|\mu|}{\Lambda_2}p_2\psi_2^{(\ell+1)}(x,\mu)-\frac{|\mu|}{\Lambda_1}p_1\psi_1^{(\ell+1)}(x,\mu)+p_1S_1 \tag{4}$$

$$\mu\frac{\partial}{\partial x}p_2\psi_2^{(\ell+1)}(x,\mu)+\sigma_2(x)\,p_2\psi_2^{(\ell+1)}(x,\mu)=\frac{\sigma_{s2}(x)}{2}\int_{-1}^{1}d\mu' p_2\psi_2^{(\ell)}\left(x,\mu'\right)$$
$$+\frac{|\mu|}{\Lambda_1}p_1\psi_1^{(\ell+1)}(x,\mu)-\frac{|\mu|}{\Lambda_2}p_2\psi_2^{(\ell+1)}(x,\mu)+p_2S_2. \tag{5}$$

These transport sweeps are similar to a "two spatial unknown per zone" slab geometry spatial discretization such as the linear discontinuous method.

2.2 Fourier Analysis

To perform a Fourier analysis, we first write an exact equation for the iterative error by subtracting (4) and (5) from the converged system:

$$\mu\frac{\partial}{\partial x}p_1\varepsilon_1^{(\ell+1)}(x,\mu)+\sigma_1(x)\,p_1\varepsilon_1^{(\ell+1)}(x,\mu)$$
$$=\frac{\sigma_{s1}(x)}{2}\int_{-1}^{1}d\mu' p_1\varepsilon_1^{(\ell)}(x,\mu')+\frac{|\mu|}{\Lambda_2}p_2\varepsilon_2^{(\ell+1)}(x,\mu)-\frac{|\mu|}{\Lambda_1}p_1\varepsilon_1^{(\ell+1)}(x,\mu) \tag{6}$$

$$\mu\frac{\partial}{\partial x}p_2\varepsilon_2^{(\ell+1)}(x,\mu)+\sigma_2(x)\,p_2\varepsilon_2^{(\ell+1)}(x,\mu)$$
$$=\frac{\sigma_{s2}(x)}{2}\int_{-1}^{1}d\mu' p_2\varepsilon_2^{(\ell)}(x,\mu')+\frac{|\mu|}{\Lambda_1}p_1\varepsilon_1^{(\ell+1)}(x,\mu)-\frac{|\mu|}{\Lambda_2}p_2\varepsilon_2^{(\ell+1)}(x,\mu) \tag{7}$$

where

$$\varepsilon_{1,2}^{(\ell+1)}(x,\mu)=\psi_{1,2}(x,\mu)-\psi_{1,2}^{(\ell+1)}(x,\mu)$$

We assume the iteration errors can be represented by the Fourier ansatz

$$p_{1,2}\varepsilon_{1,2}^{(\,)}(x,\mu)\cong\omega^{(\,)}\xi_{1,2}(\mu)\,e^{i\lambda x} \tag{8}$$

Here we have defined ω to be the iteration eigenvalues, $\xi_{1,2}(\mu)$ are the associated eigenvectors, λ is the Fourier mode frequency, and $i=\sqrt{-1}$.

Substituting this ansatz into Eqs. (6) and (7) yields the following eigensystem.

$$\omega\left[\xi_1(\mu)\left(i\mu\lambda+\sigma_1(x)+\frac{|\mu|}{\Lambda_1}\right)-\frac{|\mu|}{\Lambda_2}\xi_2(\mu)\right]=\frac{\sigma_{s1}(x)}{2}\int_{-1}^{1}d\mu'\xi_1(\mu') \tag{9}$$

$$\omega\left[\xi_2(\mu)\left(i\mu\lambda+\sigma_2(x)+\frac{|\mu|}{\Lambda_2}\right)-\frac{|\mu|}{\Lambda_1}\xi_1(\mu)\right]=\frac{\sigma_{s2}(x)}{2}\int_{-1}^{1}d\mu'\xi_2(\mu') \tag{10}$$

The eigenvalues of this system determine the rate of convergence of the iterative scheme.

2.3 Numerical Results

To motivate the development of our acceleration equations, we briefly summarize the Fourier analysis predictions for a suite of test problems. These test problems were originally described in Adams, Larsen and Pomraning (1989), and we include the data in Table 1. The problems are chosen such that the ensemble-averaged total cross-section, $\langle\sigma\rangle$, is equal to unity. [In the table, c_i is the scattering ratio in material i.]

The Fourier analysis spectral radii and observed convergence behavior for these test problems are shown in Table 2. The data in column three of this table was generated by a diamond-differenced slab-geometry transport code using the S_{16} Gauss-Legendre quadrature set. We have chosen a slab length of 100 *cm* with vacuum boundaries and no interior sources. The initial flux in each material is random, to excite all the available error modes.

Test Problem #	σ_1	c_1	Λ_1	σ_2	c_2	Λ_2
1	10/99	0.0	99/100	100/11	1.0	11/100
2	10/99	1.0	99/100	100/11	0.0	11/100
3	10/99	0.9	99/100	100/11	0.9	11/100
4	10/99	0.0	99/10	100/11	1.0	11/10
5	10/99	1.0	99/10	100/11	0.0	11/10
6	10/99	0.9	99/10	100/11	0.9	11/10
7	2/101	0.0	101/20	200/101	1.0	101/20
8	2/101	1.0	101/20	200/101	0.0	101/20
9	2/101	0.9	101/20	200/101	0.9	101/20

Table 1: Material data for the nine test problems.

Test Problem #	theoretical ρ	computational ρ
1	0.928597	0.92787
2	0.285983	0.28478
3	0.899999	0.89904
4	0.970257	0.96987
5	0.702576	0.69553
6	0.899999	0.89858
7	0.992350	0.99144
8	0.235140	0.23105
9	0.899999	0.89860

Table 2: Source Iteration spectral radii.

The slowest convergence ($\rho > 0.99$) is found in test problem 7, but there are a number of problems for which the spectral radius is 0.9 or above. Clearly, an acceleration procedure will be needed for some problems, particularly those having materials with substantially different mean chord lengths.

Figure 1 is a plot of the magnitude of the maximum eigenvalue as a function of Fourier mode λ, for the cases where the spectral radius was greater than or equal to 0.9.

This figure shows that in all of these cases (and for many more not specifically described in this paper) the largest eigenvalue occurs at $\lambda = 0$, the "flat" mode. We will let this result guide us in deriving our acceleration equations. We note here that, for some problems, there are many Fourier modes which have eigenvalues approaching unity, which may cause the performance of the acceleration equations to degrade.

3. A "MIXED" TRANSPORT ACCELERATION SCHEME

The Fourier analysis results in the previous section indicate that the slowest converging SI error modes are spatially flat. This is analgous to the results of a Fourier analysis of multigroup transport with upscattering. Adams and Morel (1993) showed that the solution of an infinite medium problem could be used as a spectrum for collapsing the multigroup transport equations to a one group diffusion equation. This diffusion equation makes a very effective preconditioner for the multigroup source iteration.

We use the same idea here. Our BSM transport equations look very much like a two-group transport problem with angle-dependent upscattering. We will solve an infinite medium BSM equation to generate a weighting function which can then be used to collapse our BSM equations to a single "mixed" transport equation. This weighting function is the eigenfunction corresponding to the largest Source Iteration eigenvalue, and is designed to eliminate the "flat" mode of the solution. The mixed transport equation will be driven by a weighted average of the SI residual in each of the two materials and will provide a correction to the SI flux solution.

3.1 Derivation of the Acceleration Equations

To derive the acceleration equations, we begin by adding the two SI equations for iteration errors (Eqs. 6 and 7):

$$\mu\frac{\partial}{\partial x}\left[p_1\varepsilon_1^{(\ell+1/2)}(\mu)+p_2\varepsilon_2^{(\ell+1/2)}(\mu)\right]+\sigma_1 p_1\varepsilon_1^{(\ell+1/2)}(\mu)+\sigma_2 p_2\varepsilon_2^{(\ell+1/2)}(\mu)$$
$$=\frac{\sigma_{s1}}{2}\int_{-1}^{1}d\mu' p_1\varepsilon_1^{(\ell)}(\mu')+\frac{\sigma_{s2}}{2}\int_{-1}^{1}d\mu' p_2\varepsilon_2^{(\ell)}(\mu'). \qquad (11)$$

We next assume that the iteration error in each material can be represented as product of a single space-dependent modulation function, $\Upsilon_{eff}(x,\mu)$, and a spectral shape $\xi_{1,2}(\mu)$ function such that:

$$p_{(1,2)}\ \varepsilon_{(1,2)}^{(\ell+1/2)}(x,\mu)=\Upsilon_{eff}^{(\ell+1/2)}(x,\mu)\ \xi_{(1,2)}(\mu), \qquad (12)$$

where the spectral shape function is normalized in the following way:

$$\xi_1(\mu)+\xi_2(\mu)=1. \qquad (13)$$

The spectral shape function is defined to be the eigenvector, corresponding to the maximum eigenvalue of the SI operator (the $\lambda=0$ mode).

Substituting Eq. (12) into Eq. (11) yields

$$\mu\frac{\partial}{\partial x}\Upsilon_{eff}^{(\ell+1/2)}(x,\mu)+\left[\sigma_1\xi_1(\mu)+\sigma_2\xi_2(\mu)\right]\Upsilon_{eff}^{(\ell+1/2)}(x,\mu)$$
$$=\frac{\sigma_{s1}}{2}\int_{-1}^{1}p_1\varepsilon_1^{(\ell)}(x,\mu')\,d\mu'+\frac{\sigma_{s2}}{2}\int_{-1}^{1}p_2\varepsilon_2^{(\ell)}(x,\mu')\,d\mu'. \qquad (14)$$

or, in terms of Source Iteration residuals,

$$\mu\frac{\partial}{\partial x}\Upsilon_{eff}^{(\ell+1/2)}(x,\mu)+\sigma_{eff}(\mu)\Upsilon_{eff}^{(\ell+1/2)}(x,\mu)$$
$$=\frac{\sigma_{s,eff}(\mu)}{2}\int_{-1}^{1}d\mu'\Upsilon_{eff}^{(\ell+1/2)}(x,\mu')+\frac{R_1^{(\ell+1/2)}(x)}{2}+\frac{R_2^{(\ell+1/2)}(x)}{2}. \qquad (15)$$

We have introduced residual terms $R_{(1,2)}^{(\ell+1/2)}$, defined by

$$R_{(1,2)}^{(\ell+1/2)}(x) = \sigma_{s(1,2)} p_{(1,2)} \left[\phi_{(1,2)}^{(\ell+1/2)}(x) - \phi_{(1,2)}^{(\ell)}(x) \right], \tag{16}$$

and angle-dependent "effective" cross-sections of the form

$$\sigma_{eff}(\mu) = \sigma_1 \xi_1(\mu) + \sigma_2 \xi_2(\mu), \tag{17}$$

$$\sigma_{s,eff}(\mu) = \sigma_{s1} \xi_1(\mu) + \sigma_{s2} \xi_2(\mu). \tag{18}$$

Eq. (15) yields a correction to the "mixed" angular flux. This correction can then be applied to the scalar flux in each material:

$$\phi_{(1,2)}^{(\ell+1)}(x) = \phi_{(1,2)}^{(\ell+1/2)}(x) + \int_{-1}^{1} d\mu' \Upsilon_{eff}^{(\ell+1/2)}(x,\mu') \; \xi_{1,2}(\mu') \tag{19}$$

Equations (6), (7), (15), and (19) completely define our acceleration procedure.

3.2 Fourier Analysis

The Fourier analysis process begins with a choice of Fourier ansatz:

$$p_{(1,2)} \varepsilon_{(1,2)}^{(\ell)}(x,\mu) \cong \omega^{(\ell)} \xi_{(1,2)}(\mu) e^{i\lambda x} \tag{20}$$

$$p_{(1,2)} \varepsilon_{(1,2)}^{(\ell+1/2)}(x,\mu) \cong \omega^{(\ell)} \Psi_{(1,2)}(\mu) e^{i\lambda x} \tag{21}$$

$$\Upsilon_{eff}^{(\ell+1/2)}(x,\mu) \cong \omega^{(\ell)} \xi_{eff}(\mu) e^{i\lambda x}, \tag{22}$$

$$E_{(1,2)} = \int_{-1}^{1} \xi_{(1,2)}(\mu') \, d\mu' \tag{23}$$

$$\Phi_{(1,2)} = \int_{-1}^{1} \Psi_{(1,2)}(\mu') \, d\mu' \, . \tag{24}$$

Substituting the ansatz into the coupled transport sweep equations gives the following matrix equation:

$$\mathbf{P} = \mathbf{L}\,\mathbf{S}\,\mathbf{E}, \tag{25}$$

where we have defined

$$\mathbf{L} = \sum_m w_m \begin{bmatrix} i\mu_m\lambda + \sigma_1 + \frac{|\mu_m|}{\Lambda_1} & -\frac{|\mu_m|}{\Lambda_2} \\ -\frac{|\mu_m|}{\Lambda_1} & i\mu_m\lambda + \sigma_2 + \frac{|\mu_m|}{\Lambda_2} \end{bmatrix}^{-1}, \tag{26}$$

$$\mathbf{S} = \begin{bmatrix} \frac{\sigma_{s1}}{2} & 0 \\ 0 & \frac{\sigma_{s2}}{2} \end{bmatrix}, \tag{27}$$

$$\mathbf{E} = \begin{bmatrix} E_1 \\ E_2 \end{bmatrix}, \tag{28}$$

$$\mathbf{P} = \begin{bmatrix} \Phi_1 \\ \Phi_2 \end{bmatrix}. \tag{29}$$

After inserting the ansatz into the mixed transport acceleration equation and the update equation, we obtain the following eigensystem for the accelerated iteration procedure:

$$\omega \mathbf{E} = \left[\mathbf{L}\,\mathbf{S} + \mathbf{G}\,\mathbf{L}_{\mathbf{eff}}^{-\mathbf{1}}\,\mathbf{B}\,(\mathbf{L}\,\mathbf{S} - \mathbf{I}) \right] \mathbf{E} \tag{30}$$

with the associated matrix definitions:

$$\mathbf{L_{eff}} = \begin{bmatrix} i\lambda\mu_1 + \sigma_{eff}(\mu_1) & \cdots & 0 \\ \vdots & \ddots & \vdots \\ 0 & \cdots & i\lambda\mu_N + \sigma_{eff}(\mu_N) \end{bmatrix}_{N\times N} - \frac{1}{2} \begin{bmatrix} \sigma_{s,eff}(\mu_1)w_1 & \cdots & \sigma_{s,eff}(\mu_N)w_N \\ \vdots & \vdots & \vdots \\ \sigma_{s,eff}(\mu_1)w_1 & \cdots & \sigma_{s,eff}(\mu_N)w_N \end{bmatrix}_{N\times N}, \tag{31}$$

$$\mathbf{B} = \begin{bmatrix} 1 & 1 \\ \vdots & \vdots \\ 1 & 1 \end{bmatrix}_{N\times 2}, \tag{32}$$

$$\mathbf{G} = \begin{bmatrix} w_1\xi_1(\mu_1) & w_2\xi_1(\mu_2) & \cdots & w_N\xi_1(\mu_N) \\ w_1\xi_2(\mu_1) & w_2\xi_2(\mu_2) & \cdots & w_N\xi_2(\mu_N) \end{bmatrix}_{2\times N}. \tag{33}$$

3.3 Acceleration Results

In examining the effectiveness of this acceleration scheme, we first focus on the "flat" error modes. If the acceleration equations are functioning properly, the largest of the two eigenvalues for $\lambda = 0$ will be reduced to zero. Table 3 compares the largest (in magnitude) eigenvalue for the flat mode. In six of the test problems, the maximum eigenvalue is reduced to nearly zero. In all nine problems the accelerated flat mode eigenvalue is smaller than the minimum of the two unaccelerated eigenvalues. For all the test problems (and for many other test problems not described in detail here) the maximum flat mode eigenvalue is smaller in the accelerated system than in the unaccelerated system.

In Figure 2, we plot the maximum eigenvalue of SI and the accelerated iteration scheme as a function of Fourier mode frequency for test problems 1, 4 and 7. It is clear that the acceleration scheme is working very well for the low-frequency error modes, and in fact, also seems to be effective at improving the convergence of the higher frequency modes.

Table 4 compares the spectral radii for the accelerated system (from the Fourier analysis and from observations of the implemented algorithm) and the unaccelerated system. All the results in this section were generated with the S_4 Gauss-Legendre angular quadrature set.

There are three important conclusions to be drawn from this data. First, the Fourier analysis results compare well with the observed convergence behavior. The 100 *cm*-thick

Test Problem #	unaccelerated $\|\omega\|$	accelerated $\|\omega\|$
1	0.924619	0.003298
2	0.246187	0.000006
3	0.900000	0.153725
4	0.968480	0.044110
5	0.684799	0.000003
6	0.900000	0.587951
7	0.991910	0.001008
8	0.191045	0.000011
9	0.900000	0.164660

Table 3: Eigenvalues at $\lambda = 0$ with and without acceleration

slab used to generate the fourth column of data is a reasonable approximation of an infinite medium for most of the test problems. Second, the spectral radii for the acceleration scheme are smaller than those of Source Iteration for all the test problems. Third, the acceleration scheme yields a maximum spectral radius of approximately 0.76 for the materials considered in the nine test problems.

Test Problem #	unaccelerated theoretical ρ	accelerated theoretical ρ	accelerated computational ρ	relative error [%]:
1	0.924619	0.560205	0.54591	-2.55174
2	0.246187	0.002989	0.00237	-20.70927
3	0.900000	0.518922	0.49588	-4.44036
4	0.968480	0.762446	0.75921	-0.42442
5	0.684799	0.002635	0.00171	-35.10436
6	0.900000	0.763959	0.75565	-1.08762
7	0.991910	0.695584	0.68711	-1.21826
8	0.191045	0.004105	0.00312	-23.99513
9	0.900000	0.405868	0.38535	-5.05534

Table 4: Spectral radii of the acceleration scheme.

While the "mixed" transport equation we have derived appears to be an effective accelerator for the coupled BSM transport equations solved with Source Iteration, it is important to recognize that iterations on the "mixed" scattering source will be necessary to solve the acceleration equations. We address this concern in the next section.

4. DSA FOR THE LOW-ORDER "MIXED" TRANSPORT EQUATION

In the analysis presented in the previous section, we assumed that the "mixed" transport acceleration equation was completely converged. However, since this is a transport equation with scattering, we must iterate to find its solution. Source Iteration will also converge slowly here if the effective scattering ratio is near unity. It will be necessary to accelerate the convergence of the iterations on this low-order transport equation.

In this section, we derive diffusion synthetic acceleration equations for the "mixed" transport equation using the Four-Step method of Larsen (1982). We then Fourier analyze the technique and present predicted and observed spectral radii.

4.1 Derivation of the acceleration equations

To derive the DSA system, we apply Larsen's 4-step procedure:

1. Write the discretized transport equation for the error at iteration step $(\ell+1)$.
2. Take the 0th angular moment of the discretized transport equation.
3. Take the 1st angular moment of the discretized transport equation.
4. Eliminate the first moments from the resulting system, leaving a discretized diffusion equation for the scalar fluxes.

If we apply this procedure to the analytic-in-space mixed transport equation, we obtain the following diffusion equation for a correction:

$$-\frac{\partial}{\partial x}\frac{1}{3\sigma_{eff,2}}\frac{\partial}{\partial x}F^{(\alpha+1)}(x)+\sigma_{a,eff,0}F^{(\alpha+1)}(x) = \int_{-1}^{1}\sigma_{s,eff}(\mu')\Upsilon_{eff}^{(\alpha+1/2)}(x,\mu')d\mu'-\int_{-1}^{1}\sigma_{s,eff}(\mu')\Upsilon_{eff}^{(\alpha)}(x,\mu')d\mu'. \tag{34}$$

where α indicates an inner iteration on the "mixed" scattering source.

In Equation 34, we have defined a 0th-moment absorption cross-section

$$\sigma_{a,eff,0}=\sigma_{eff,0}-\sigma_{s,eff,0}=\frac{\int_{-1}^{1}\sigma_{eff}(\mu')d\mu'}{\int_{-1}^{1}d\mu'}-\frac{\int_{-1}^{1}\sigma_{s,eff}(\mu')d\mu'}{\int_{-1}^{1}d\mu'}, \tag{35}$$

a 2nd-moment effective total cross-section

$$\sigma_{eff,2}=\frac{3\int_{-1}^{1}\mu'^{2}\sigma_{eff}(\mu')d\mu'}{\int_{-1}^{1}d\mu'}, \tag{36}$$

and an effective diffusion coefficient

$$D=\left[\frac{\lambda^2}{3\sigma_{eff,2}}+\sigma_{a,eff,0}\right]. \tag{37}$$

F is an additive correction to the Source Iteration scalar flux. Applying this correction gives the new estimate of the scattering reaction rate:

$$\int_{-1}^{1} \sigma_{s,eff}(\mu') \Upsilon_{eff}^{(\alpha+1)}(x,\mu') d\mu' = \int_{-1}^{1} \sigma_{s,eff}(\mu') \Upsilon_{eff}^{(\alpha+1/2)}(x,\mu') d\mu' + F^{(\alpha+1)}(x) \int_{-1}^{1} \sigma_{s,eff}(\mu') d\mu'. \quad (38)$$

4.2 Fourier Analysis

A Fourier analysis of this scheme yields the following closed form expression for the eigenvalue of the iteration operator:

$$\omega = \frac{1}{2} \int_{-1}^{1} \frac{\sigma_{s,eff}(\mu)}{i\mu\lambda + \sigma_{eff}(\mu)} d\mu + D^{-1} \sigma_{s,eff,0} \left[\frac{1}{2} \int_{-1}^{1} \frac{\sigma_{s,eff}(\mu)}{i\mu\lambda + \sigma_{eff}(\mu)} d\mu - 1 \right]. \quad (39)$$

In writing (39), we must note that we have divided out the term

$$\int_{-1}^{1} \sigma_{s,eff}(\mu') a\left(\mu'\right) d\mu', \quad (40)$$

as it is common to each term of the system.

Equation 39 is the standard result for the DSA eigenvalue, aside from the direction-averaged cross-sections.

4.3 Numerical Results

For the Fourier analysis of the coarse-grid diffusion synthetic acceleration scheme, we again use the material data from the test problems in Adams, Larsen and Pomraning (1989). As before, we discretize the angular variable using the S_4 Gauss-Legendre quadrature set.

We verify the Fourier analysis spectral radii predictions with observed convergence rates from the implemented algorithm. For the diamond-difference spatial discretization of the "mixed" transport equation, the application of the Four-Step procedure yields the well-known [Larsen (1982)] discretized diffusion equation, with the added wrinkle of "direction-averaged" cross-sections:

$$-\frac{1}{3\Delta x \sigma_{eff,2}} \left[F_{k+3/2}^{(\alpha+1)} - F_{k+1/2}^{(\alpha+1)} \right] + \frac{1}{3\Delta x \sigma_{eff,2}} \left[F_{k+1/2}^{(\alpha+1)} - F_{k-1/2}^{(\alpha+1)} \right] + \frac{1}{4} \Delta x \sigma_{a,eff,0} F_{k+3/2}^{(\alpha+1)} + \frac{1}{2} \Delta x \sigma_{a,eff,0} F_{k+1/2}^{(\alpha+1)} + \frac{1}{4} \Delta x \sigma_{a,eff,0} F_{k-1/2}^{(\alpha+1)} = \frac{1}{2} \Delta x \left(\Theta_k^{(\alpha+1/2)} + \Theta_{k+1}^{(\alpha+1/2)} \right). \quad (41)$$

[In these equations, the mesh spacing and material properties are assumed to be uniform.]

We note that (41) is a three-point stencil for correction factors, F, at cell-edges $k-1/2$, $k+1/2$, and $k+3/2$. A variety of linear solvers could be employed to solve this tridiagonal system. The resulting correction factors, $F_k^{(\alpha+1)}$, are then used to correct and update

$\Upsilon_{eff,k,m}^{(\alpha+1)}$

$$\sum_{m=1}^{N} w_m \sigma_{s,eff,m} \Upsilon_{eff,k,m}^{(\alpha+1)} = \sum_{m=1}^{N} w_m \sigma_{s,eff,m} \Upsilon_{eff,k,m}^{(\alpha+1/2)} + \frac{1}{2} F_k^{(\alpha+1)} \sum_{m=1}^{N} w_m \sigma_{s,eff,m}. \qquad (42)$$

Our discretized results are obtained by considering a slab of length 5000 *cm*, and we again run the zero-source problem with a random initial guess to best compare with the Fourier analysis. Table 5 contains results from the implemented DSA scheme compared with the Fourier analysis. The deviations from predicted behavior, most noticeably in test problems 2 and 5, are due in part to errors from the outer iteration on the coupled transport system. All the finite slab spectral radii are below those predicted by Fourier analysis, as they should be for these model problems.

Table 5: Performance of the coarse-grid DSA scheme

Test Problem #	accelerated theoretical ρ	accelerated computational ρ	relative error [%]
1	0.180038	0.17282	-4.00915
2	0.025340	0.01470	-41.98895
3	0.153975	0.14665	-4.75727
4	0.237271	0.22913	-3.43110
5	0.096444	0.05254	-45.52279
6	0.153975	0.14665	-4.75727
7	0.192683	0.18496	-4.00814
8	0.024467	0.02446	-0.02861
9	0.153975	0.14781	-4.00390

5. DISCUSSION AND CONCLUSIONS

We have successfully derived and tested an acceleration scheme for the BSM transport equations. Our Fourier analyses do not provide closed-form expressions for the spectral radii, but have tried to gain some information on the trends in convergence behavior.

While this paper focuses strictly on stochastic mixtures of two Markovian materials using the Levermore-Pomraning mix model, our methodology can be extended to more general situations. For mixtures of N materials, the coupled transport equations have the form of an N group transport problem with a general upscattering operator. The formulation presented here can handle this case. Non-Markovian statistics can be incorporated provided the material interface terms are linear combinations of the material ensemble-average angular fluxes. Higher order coupling models, such as that of Su and Pomraning (1995) cannot be accelerated with this new iteration scheme, unless modifications are made.

One obvious extension of this work is the potential for applying the mixed DSA equation derived in Section 4 directly to the acceleration of the coupled BSM transport

equations. We are currently generating Fourier analysis results for this acceleration technique and will be reporting them in the near future.

Another possible outcome of this research is the use of either the mixed low-order transport or DSA equation as an approximate model of BSM transport. We would like to answer the following question: under what conditions do the "mixed" acceleration equations yield results which accurately approximate that of the coupled BSM equations? This research is also currently ongoing.

A major area of research which is currently unexplored is the computation of two- and three-dimensional BSM transport solutions. We are unaware of any research which compares the solutions of multi-dimensional benchmark problems to Levermore-Pomraning model results. In the future, this will be crucial in the application of stochastic mix models to realistic problems.

ACKNOWLEDGMENTS

In the completion of this work, we received valuable comments and suggestions from Marvin Adams, Edward Larsen, Mike Zika, Frank Graziani and David Miller. We would also like to formally express our appreciation to Jerry Pomraning, whose technical accomplishments laid the groundwork for this research, and whose personality and dedication to this field sparked our desire to learn more about it.

REFERENCES

Adams, B.T., Morel, J.E., 1993. A Two-Grid Acceleration Scheme for the Multigroup S_n Equations with Neutron Upscattering, *Nucl. Sci. Eng.*, **115**, 253.

Adams, M.L., Larsen, E.W., Pomraning, G.C., 1989. Benchmark Results for Particle Transport in a Binary Markov Statistical Medium, *JQSRT* **42**, 253.

Audic, S., Frisch, H., 1993. Monte-Carlo Simulation of a Radiative Transfer Problem in a Random Medium: Application to a Binary Mixture, *JQSRT*, **50**, 127.

Ching, B.S., Palmer, T.S., 2000. Analysis of Iterative Schemes for Binary Stochastic Mixture Transport Equations, *Trans. Am. Nucl. Soc.*, **82**, 148.

Larsen, E.W., 1982. Unconditionally Stable Diffusion-Synthetic Accleration Methods for the Slab Geometry Discrete Ordinates Equations, Part I: Theory, *Nucl. Sci. Eng.*, **82**, 47.

Malvagi, F., Pomraning, G.C., 1992. A Comparison of Models for Particle Transport Through Stochastic Mixtures, *Nucl. Sci. Eng.*, **111**, 215.

Miller, D.S., 2001. Benchmarks and Models for Time-Dependent Grey Radiation Transport with Material Temperature in Binary Stochastic Mixtures, *JQSRT*, to appear.

Miller, D.S., Rodrigue, G., Graziani, F., 2001. A Convergence Analysis of Source Iteration for the Solution of Coupled Transport Equations on a Stochastic Media, UCRL-JC-141985.

Su, B., Pomraning, G.C., 1993. Benchmark Results for Particle Transport in Binary Non-Markovian Mixtures, *JQSRT*, **50**, 211.

Su, B., Pomraning, G.C., 1995. Modification to a Previous Higher Order Model for Particle Transport in Binary Stochastic Media, *JQSRT*, **54**, 779.

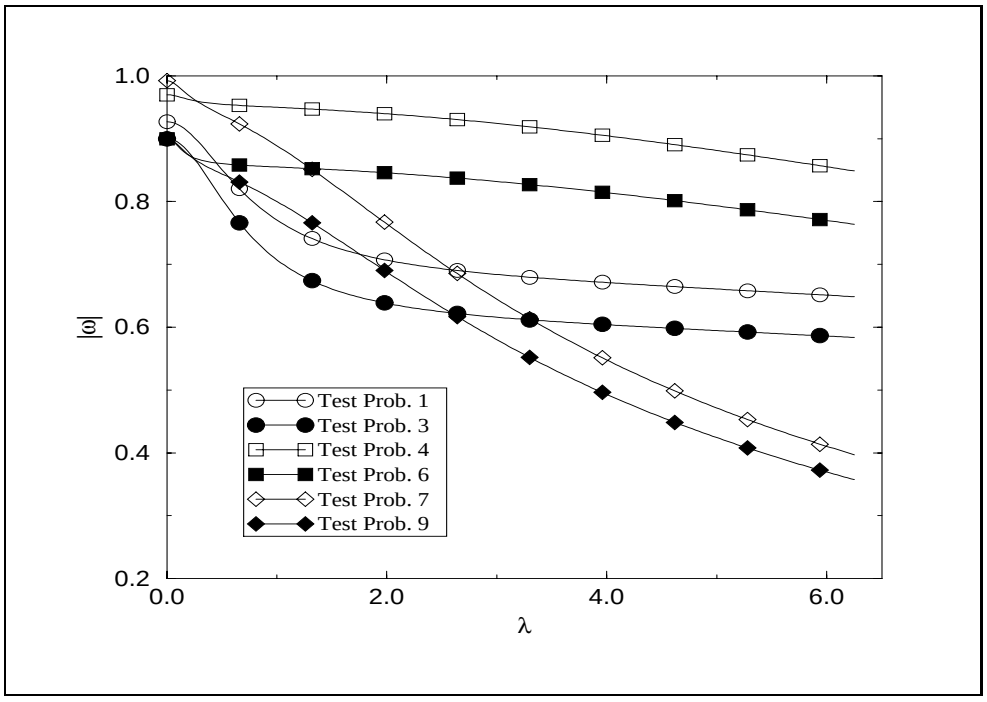

Fig. 1: Source iteration eigenvalues for test problems 1, 3, 4, 6, 7 and 9.

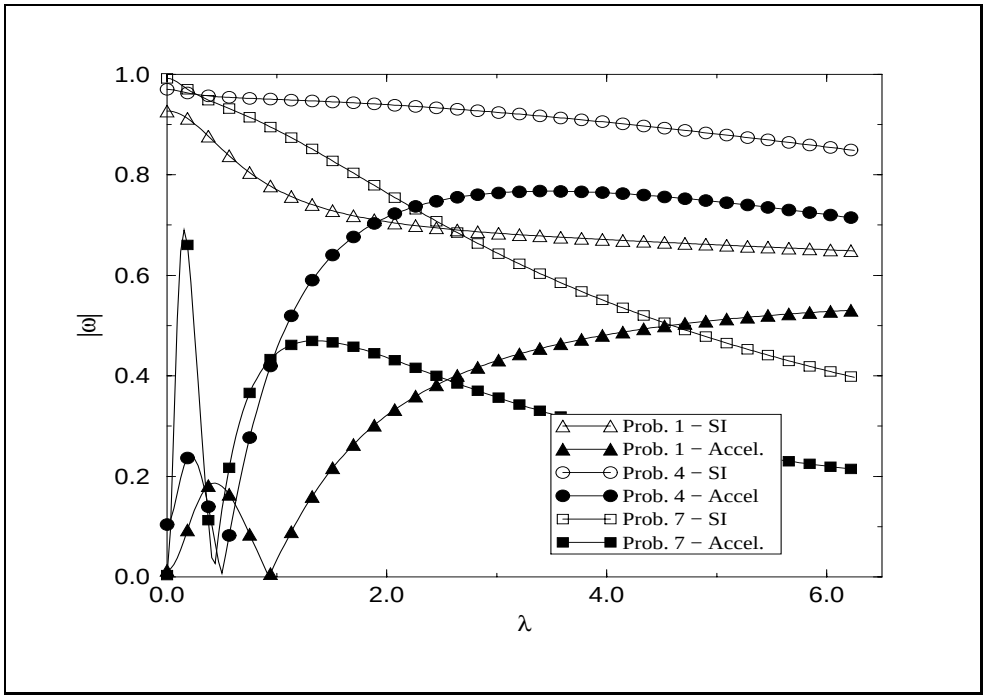

Fig. 2: SI and accelerated eigenvalues for test problems 1, 4 and 7